JOURNAL OF BACTERIOLOGY, Sept. 1975, p. 1184-1196

Vol. 123, No. 3
Printed in U.S.A.

Study of Cell Wall Growth in *Bacillus megaterium* by High-Resolution Autoradiography

CHANTAL DE CHASTELLIER, RAYMOND HELLIO, AND ANTOINETTE RYTER*
Unité de Microscopie Electronique, Département de Biologie Moléculaire, Institut Pasteur, 75015 Paris, France

Received for publication 3 April 1975

Growth of the cell wall of *Bacillus megaterium* was studied by pulse-labeling the cell wall of a DAP⁻ Lys⁻ mutant for a very short time with tritium-labeled diaminopimelic acid. The distribution of radioactivity along the cell wall was examined by high-resolution autoradiography on isolated cell walls and thin sections of bacteria. The results indicate that cell wall elongation occurs by diffuse intercalation of newly synthesized murein into the expanding cell wall during exponential growth, as well as during germination, and that the only zone of highly localized diaminopimelic acid incorporation is found at the cross wall during its synthesis. This zone contains about 30% of the radioactivity incorporated into the cell wall. Analysis of autoradiographs of thin sections of bacteria shows that the total radioactivity incorporated per bacterium doubles during the life cycle. This doubling occurs in the cylindrical part of the cell wall but not in the polar caps. This seems to indicate that elongation of the bacterium is not constant during the life cycle but increases with the length of the cell.

Many attempts have been made by different morphological approaches to determine the growth pattern of the cell wall of gram-positive bacteria. In spherical bacteria, whatever type of labeling used, all studies have shown a unique growth zone located at the cell equator, responsible for cross wall formation as well as elongation of the cell wall (3, 10, 11, 18, 19, 33, 34). The situation remains, however, more ambiguous for rod-shaped bacteria. Some authors find discrete growth zones (9, 22) whereas many others conclude in favor of diffuse growth (2, 8, 15, 20, 21, 25, 26). These discrepancies could be due to the high turnover of cell wall constituents observed in rod-shaped species (5-7, 24) and perhaps also to a continuous rearrangement of mucopeptides as found in *Escherichia coli* (29). These two phenomena could mask zonal growth, especially when observations are made on fully labeled bacteria submitted to a prolonged chase in the absence of marker, as was the case for all morphological studies done until now.

It was therefore important to determine the cell wall growth pattern after very short pulse-labelings as recently was done for *E. coli* (29). A mutant of *Bacillus megaterium* requiring diaminopimelic acid (DAP) and lysine for growth was therefore pulse-labeled with tritiated DAP for 0.025 or 0.05 of the generation time during exponential growth and spore germination. The localization of radioactive DAP molecules incorporated into the cell wall was studied by high-resolution autoradiography with the electron microscope either on isolated cell walls or on thin sections of bacteria.

MATERIALS AND METHODS

Strain and medium. Labeling experiments were done during exponential growth or germination with a DAP⁻ Lys⁻ mutant of *B. megaterium* isolated from the strain MB. The latter, already used in previous studies (15), was chosen because it makes small chains of two cells only instead of the usual long chains. This greatly facilitates morphological observations of cell wall growth.

Bacteria were grown at 30 C with aeration in Salton synthetic medium (1) supplemented with 1% yeast extract, 0.2% glucose, and 50 μg of DAP per ml. Under these conditions the doubling time is 35 to 40 min.

Pulse-labeling experiments. (i) Labeling of bacteria for autoradiography on isolated cell walls. Bacteria were grown as described previously to a cell titer of about 10^8/ml. After centrifugation the pellet was resuspended in the same volume of DAP-free medium. Aliquots (5 ml) were incubated at 30 C for 30 s, 1 min, and 2 min, respectively, with 0.08 mCi of ^{3}H-labeled DAP/ml (specific activity 25 Ci/mM, Service des Molécules Marquées, C.E.A., France). The concentration of radioactive DAP was therefore 0.6 μg/ml. Labeling was stopped with 100 μg of unlabeled DAP per ml and the samples were transferred to ice to stop the autolytic enzymes from acting upon the cell wall. As a control, an aliquot was labeled with the same concentration of ^{3}H-labeled DAP and immediately transferred to ice. All the samples were

then centrifuged and washed in Salton synthetic medium and the pellet was resuspended in Salton synthetic medium. Cell walls were obtained by mechanical breaking of bacteria in a Mickle apparatus (Laboratory Engineering Co.). The previous manipulations were all done at 0 C. After a 5-min boiling at 100 C to destroy the autolytic enzymes, the cell walls were collected by centrifugation and concentrated.

For autoradiography on whole cell walls, drops of the concentrated suspension were spread on gelatin and collodion-coated glass slides. After sublimation at −20 C, the cell walls were stained with uranyl acetate and covered with a thin coat of carbon. For autoradiography on thin sections of cell walls, the suspension was prefixed with 0.2% osmium tetroxide and then treated as described below.

(ii) Labeling of bacteria for autoradiography on thin sections. Bacteria in exponential phase were grown at 30 C with aeration in complex medium to a cell titer of 2×10^8/ml. The culture was centrifuged and the pellet was resuspended in DAP-free complex medium. A 5-ml aliquot was incubated at 30 C for 2 min with 0.12 mCi of ^{3}H-labeled DAP/ml. The concentration of radioactive DAP was therefore 0.9 μg/ml. Labeling was stopped with 250 μg of unlabeled DAP per ml and the cells were immediately prefixed with 0.2% osmium tetroxide. They were then treated as described below.

Pulse-labeling experiments were done on germinating cells in the same way as for exponentially growing cells.

Electron microscopy and autoradiography. (i) Fixation, embedding, and thin sections. The prefixed bacteria or cell walls were fixed with 1% osmium tetroxide, as described by Ryter and Kellenberger (30), dehydrated, and embedded in Epon (23). After polymerization the blocks were cut with a diamond knife on a Sorvall or Reichert ultramicrotome. For autoradiography, the thin sections were deposited on collodion-coated glass slides (16). They were stained with uranyl acetate and lead citrate (28) and covered with a thin coat of carbon.

(ii) Autoradiography. The glass slides were overlayed with photographic emulsion (1 part Ilford L4 plus 2 parts distilled water) and exposed in the dark room for 10 to 50 days depending on the radioactivity of samples. They were then developed with the physical developer of Caro (4) and dried. The collodion film was floated on distilled water and collected on supporting grids. Because of poor contrast whole cell walls had to be restained with uranyl acetate after dissolving the collodion with isoamyl acetate.

(iii) Data analysis of autoradiograms. The silver grain distribution on whole cell walls was analyzed on electron micrographs enlarged 10,000 times. The length of the cell walls and the position of each silver grain were determined semi-automatically with a coordinatograph, made at the Institut Pasteur, connected to a PDP-8 computer (U. Schwarz, A. Ryter, A. Rambach, R. Hellio, and Y. Hirota, submitted for publication). Data were compiled and processed to separate cell walls into three classes, according to their length, and give the numerical distribution of silver grains with respect to their distance from the center of the cell walls (i.e., transversal axis of symmetry).

The distribution of silver grains on thin sections was determined on micrographs enlarged 30,000 times. Exponentially growing bacteria were divided into four classes according to their stage in the division cycle (see Table 2). Germinating cells were divided into three classes according to their length. In all cases distances between silver grains and the chosen reference markers were measured with a ruler. Silver grain distributions along the cell wall are given in histograms.

RESULTS

Autoradiography of whole isolated cell walls. Cell walls of bacteria labeled for 1 min with ^{3}H-labeled DAP and analyzed after 11 days of autoradiography are shown in Fig. 1. Most of them present many silver grains in their middle but no other important incorporation zones are visible. The quantitative analysis of the silver grain distribution entirely confirms these observations. For this study, cell walls were divided into three classes according to their length (Table 1). The distance between each silver grain and the middle of the cell wall (transversal axis of symmetry) was measured. Because of the symmetry of the cell wall, silver grains at equal distance from the reference line were added and one-sided histograms were plotted in distance steps of 100 nm (1 mm at a 10,000 × enlargement). The distributions of silver grains in the cell wall thus obtained for each class size are represented in the three histograms of Fig. 2. In the three classes of cell walls a central zone of incorporation of ^{3}H-labeled DAP appeared, about 0.2 to 0.3 μm wide, on either side of the middle of cell walls; it contained approximately 30% of the total silver grains. No other zones appeared on the cylindrical part of the cell wall; labeling was homogeneous and decreasing towards the poles. Poles looked rather poorly labeled. Nonspecific labeling of the cell wall due to DAP adsorption did not occur since after 17 days of autoradiography, there were no silver grains on the control described above.

Autoradiography of thin sections of isolated cell walls. As shown below, autoradiographs of thin sections of bacteria contained many silver grains inside the cytoplasm. It therefore was necessary to establish the resolution of our autoradiographs, that is to say to determine at what distance from the cell wall silver grains could still be considered as representing DAP molecules incorporated into the cell wall. For this purpose, thin sections of

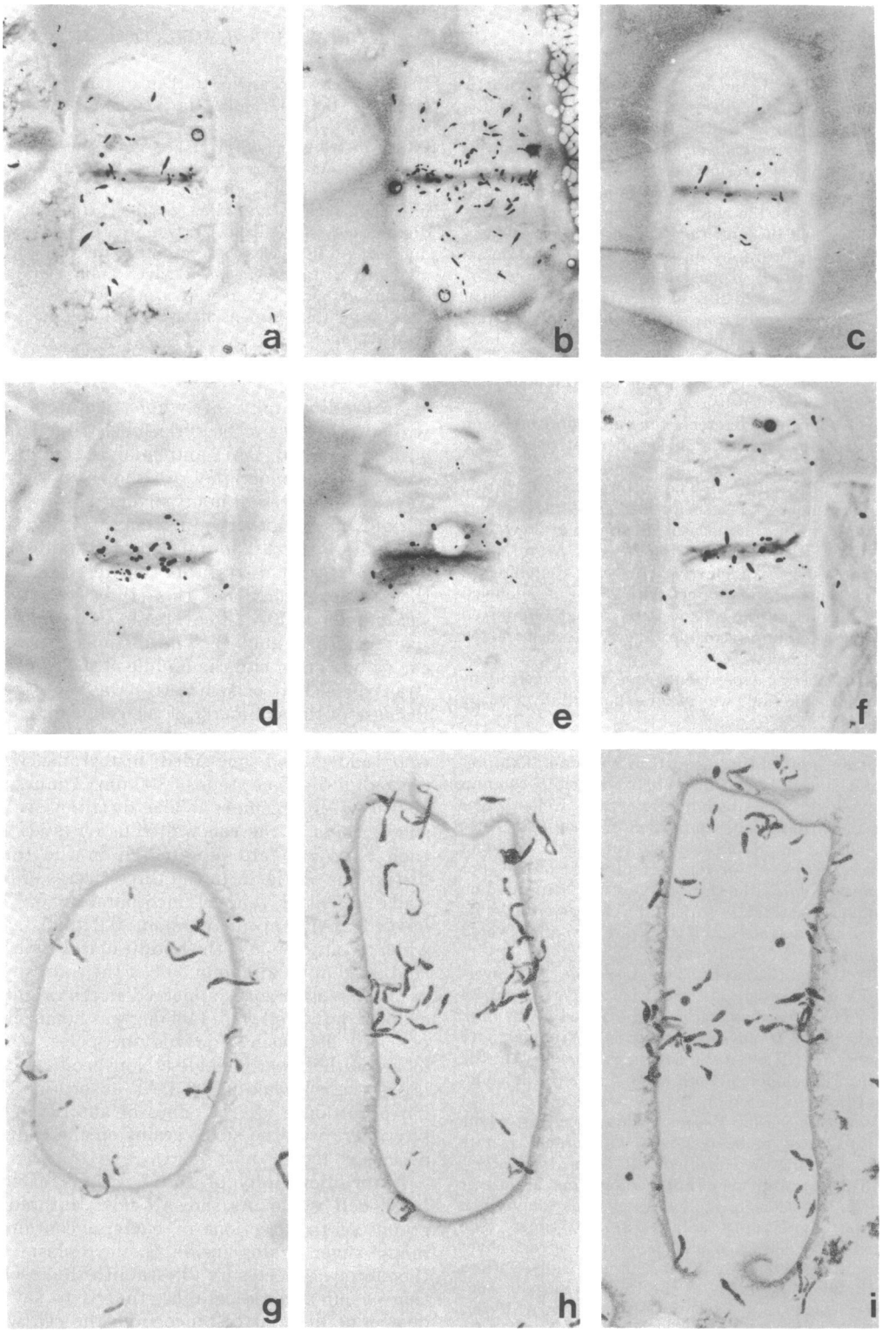

FIG. 1. *Autoradiography of whole cell walls and thin sections of cell walls isolated from bacteria labeled for 1 min with ^{3}H-labeled DAP. (a, b, c, d, e, f) Whole cell walls after 11 days of autoradiography, corresponding to the three classes of cell walls. (a, b) Class I; (c, d) class II; (e, f) class III. ×10,000. (g, h, i) Thin sections of cell walls after 50 days of autoradiography. ×24,000.*

TABLE 1. *Description of the three classes of isolated whole cell walls*[a]

Determinants	Class I	Class II	Class III
Length of cell walls (μm)	3.4-4.0	4.1-4.6	4.7-5.4
No. of cell walls analyzed	40	47	32
Total no. of silver grains considered	568	736	465

[a] The number of cell walls considered and the total number of silver grains counted in each class are given.

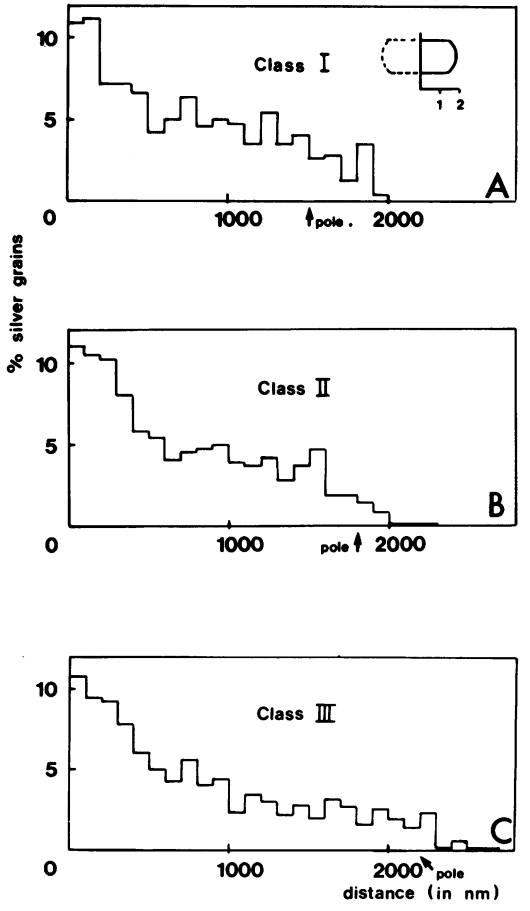

FIG. 2. *Silver grain distribution histograms with respect to the middle of whole cell walls (see insert). Cell walls (120) isolated from bacteria labeled for 1 min with* ^{3}*H-labeled DAP were analyzed after 11 days of autoradiography. These histograms were prepared in distance steps of 100 nm (1 mm at ×10,000). Quantities of silver grains are expressed as percentages of the total number of silver grains. The poles are the rounded ends of the cell wall. The arrow indicates the mean distance from the reference line at which the cell wall starts to curve. Cell walls were divided into three classes according to their length. (A) Class I; (B) class II; (C) class III.*

isolated cell walls were analyzed after 50 days of autoradiography.

Figure 1 (g, h, i) shows that the rod shape was well preserved on these thin sections. Silver grains were distributed along the cell wall and were particularly concentrated on the cross wall in formation (about 36% of the total number of silver grains). The distribution of silver grains on both sides of the cell wall was obtained by measuring the distance between silver grains and the median line of the cell wall (situated at equal distance from the inner and outer sides of the cell wall). A histogram was then plotted in distance steps of 33.3 nm (Fig. 3). It is perfectly symmetrical with respect to the reference line. These results were also tabulated in integrated form by consecutively adding the number of silver grains inside and outside the cell wall per unit distance from the median line (Fig. 4). This representation shows more clearly what fraction

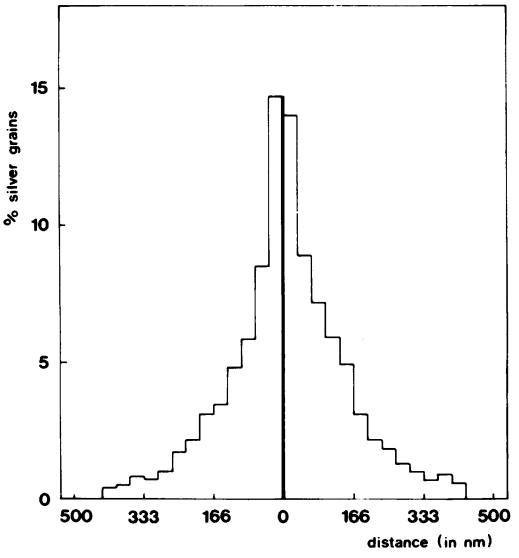

FIG. 3. *Silver grain distribution with respect to the median line of the cell wall established on thin sections of isolated cell walls. Thin sections of cell walls come from bacteria labeled for 1 min with* ^{3}*H-labeled DAP. They were analyzed after 50 days of exposition. The histogram was prepared in distance steps of 33.3 nm (1 mm at G = ×30,000). Quantities of silver grains are expressed as percentages of the total number of silver grains. Silver grains (1,450) were counted. The O axis represents the thickness of the cell wall.*

of the total number of silver grains fell within a given distance from the cell wall. It can be seen that the "half distance" (31), that is to say the distance from the median line of the cell wall within which 50% of the silver grains are found,

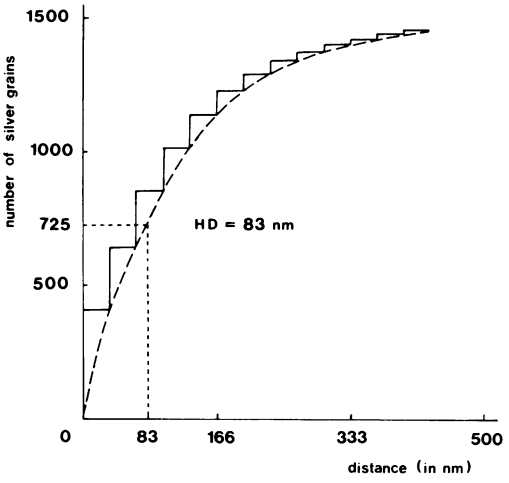

FIG. 4. *Integrated silver grain distribution histogram with respect to the median line of the cell wall established on the thin sections of cell walls described in Fig. 3. Silver grains inside and outside the cell wall were added consecutively with increasing distance from the reference line. Thus, each histogram column gives the total number of silver grains within this distance from the median line of the cell wall. Silver grains (1,450) were counted. The dotted line curve represents the curve of best fit for this histogram which was fitted by eye by joining the upper right corner of each histogram column.*

was equal to 83.3 nm (2.5 mm at a 30,000× enlargement).

Therefore, in all subsequent silver grain distribution analyses on thin sections, silver grains within 83.3 nm (2.5 mm at a 30,000× enlargement) from the median line of the cell wall, on either side, were considered as representing radioactive DAP incorporated into the cell wall.

Autoradiography of thin sections of exponentially growing bacteria. Bacteria were divided into four classes according to their division stage (Table 2). Micrographs seem to show that silver grains are uniformly distributed on the cylindrical part of the cell wall when there is no cross wall. (Fig. 5a). Then silver grains became very concentrated at the cross wall during its formation (Fig. 5b and 2), and finally reappeared evenly distributed once the cross wall was terminated and daughter cells were ready to separate (Fig. 5d). In all cases poles appeared poorly labeled, and in all classes the number of intracytoplasmic silver grains was high.

Two types of quantitative analyses were made: first, the distribution of silver grains on the different parts of the bacterium; and second, the distribution of silver grains incorporated into the cell wall as a function of their distance from the middle (i.e., the transversal axis of symmetry) of the thin section.

(i) Distribution of silver grains over the whole bacterium. A comparative study of the mean number of silver grains per thin section on the cylindrical part of the cell wall, on the cross wall, on the poles, and in the cytoplasm was done for each class of bacteria. Table 2 shows

TABLE 2. *Results of the counts of silver grains on thin sections in the different parts of exponentially growing bacteria*[a]

	Class I		Class II		Class III		Class IV			
Division stage	(1.8-2.6 μm)		(2.5-4.0 μm)		(3.0-4.8 μm)		(3.3-5.0 μm)			
							a[b]		b[c]	
	M	%	M	%	M	%	M	%	M	%
Cylindrical cell wall ...	4.58	32.13	5.36	27.15	6.50	22.50	9.42	31.74	4.71	31.74
Poles	2.58	18.10	1.32	6.70	1.67	5.90	1.40	4.78	1.70	11.52
Cross wall ...			3.20	16.20	7.50	25.90	2.00	6.74		
Cytoplasm ..	7.10	49.77	9.86	49.95	13.20	45.70	16.85	56.74	8.42	56.74

[a] Results show mean (M) number of silver grains or percentage of the total. Number of thin sections analyzed: class I, 31; class II, 56; class III, 30; class IVa, 12; class IVb, 24. Number of silver grains considered: class I, 442; class II, 1,105; class III, 866; class IVa, 356; class IVb, 356.

[b] Single cells.

[c] Two daughter cells ready to separate.

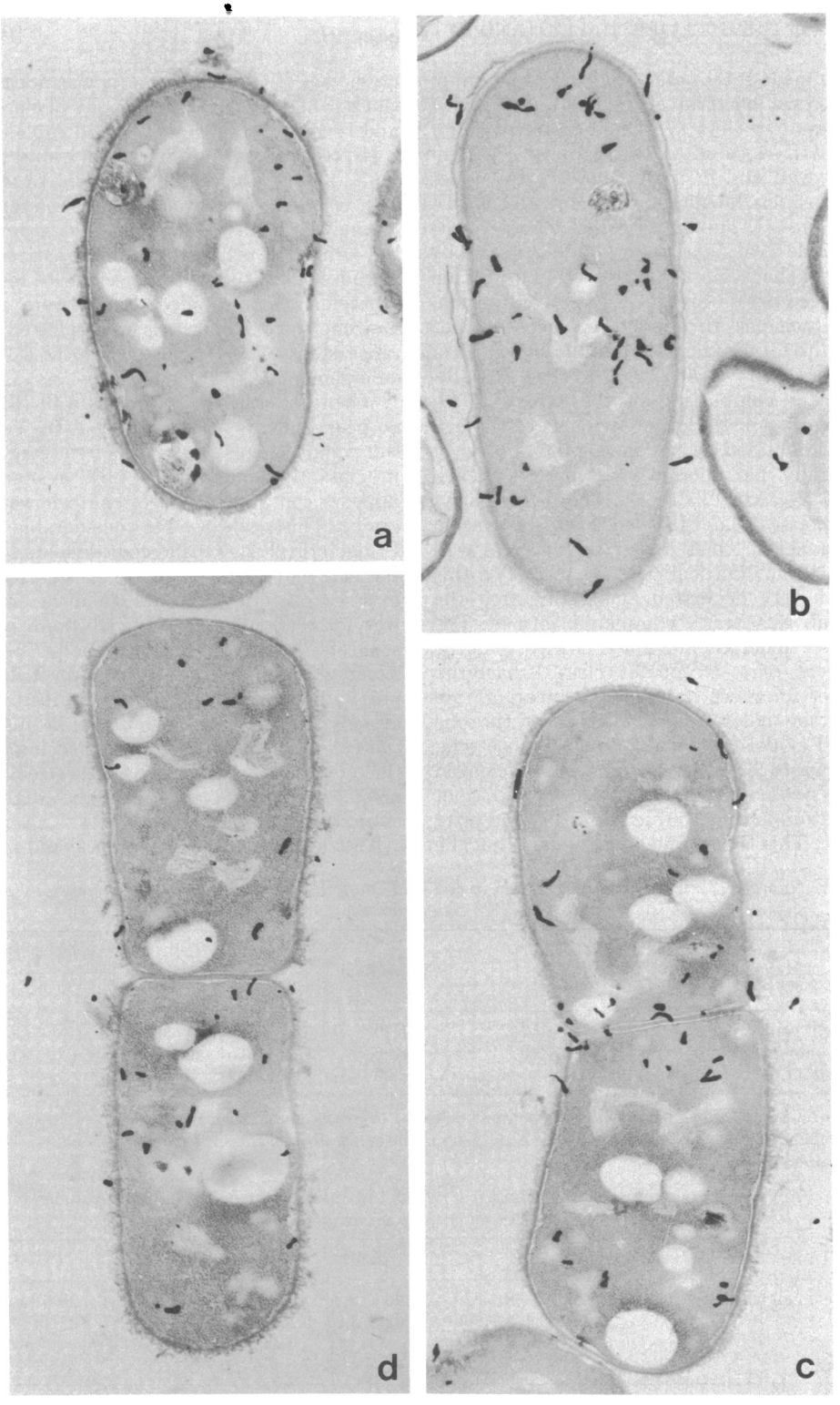

FIG. 5. *Autoradiography of longitudinal thin sections of exponentially growing bacteria labeled for 2 min with ^{3}H-labeled DAP (32 days of exposition). These micrographs correspond to the four different classes determined according to their stage in the division cycle. (a) Class I; (b) class II; (c) class III; (d) class IV. ×20,000.*

that the mean total radioactivity per bacterium increased as bacteria elongated and doubled from class I to class IV. This occurred also for radioactivity located on the cylindrical part of the cell wall and in the cytoplasm. But poles were much less labeled in classes II, III, and IV than in class I. The data expressed as percentages (Table 2) of silver grains found in each part of the cell show that the cross wall in formation was a very active area of DAP incorporation, especially in class III where it represented about 26% of the total radioactivity and about 50% of the radioactivity incorporated in the cell wall.

A better comparison of the rate of DAP incorporation in the different parts of the cell wall was obtained by calculating the number of silver grains per micron of cell wall, for each class of bacteria (Table 3). This table shows that in classes II and III the DAP incorporation rate was seven times higher in the cross wall than in the cylindrical part. In class IVa this rate was very decreased, suggesting that the cross wall was nearly completely formed. The poles were generally much less labeled than the cylindrical part except for class I bacteria. Moreover for these bacteria the incorporation rate at the poles was about half of the one observed at the cross wall of class IV bacteria. This suggests that when the cross wall is cleaved into two new poles, this portion of the wall is not fully mature and is completed during and after cleavage. This is confirmed by the fact that the cross wall of class IV bacteria was not twice as thick (34.9 ± 2.3 nm) as the poles of class II, III, and IV bacteria (21.8 ± 1.9 nm; Table 4).

(ii) Silver grain distribution along the cell wall. The middle of the bacterium, or the cross wall when it exists, was taken as reference line to analyze the distribution of silver grains along the cylindrical cell wall and the linearized poles. Because of the symmetry of cells with respect to the reference line, silver grains were counted and one-sided histograms were plotted in distance steps of 83.3 nm (2.5 mm at a 30,000× enlargement).

When bacteria have no cross wall (Fig. 6A), no peak appears at the center of the cell wall. But when the cross wall starts to be synthesized in class II bacteria (Fig. 6B), a sharp peak appears containing 33% of the cell wall silver grains. This peak became considerable in class III bacteria (Fig. 6C) and contained up to 48% of the cell wall silver grains. It lowered to 18% in class IV bacteria (Fig. 6D) when the cross wall was formed and daughter cells were ready to separate. Figure 6 also shows the uniformity of silver grain distribution along the cylindrical part of the cell wall. One interesting fact, already noticed in Table 2, is that in this part of the cell wall incorporation seemed lower when the cross wall was being synthesized. As for poles, they were always less labeled than the cylindrical cell wall.

This method of measurement could mask, at

TABLE 3. *Number of silver grains per micron of cell wall counted on thin sections of exponentially growing bacteria*[a]

Determinants	Class I	Class II	Class III	Class IV	
				a	b
Cylindrical well wall	1.52	1.29	1.00	1.24	1.24
Poles	1.10	0.55	0.65	0.59	0.76
Cross wall		6.46	7.47	2.36	

[a] Class IV bacteria can be considered as single cells (a) or as two daughter cells ready to separate (b). The total number of silver grains counted in each class along the cell wall was: class I, 222; class II, 553; class III, 470; class IV, 154.

TABLE 4. *Thickness (nanometers) of the cylindrical part of the cell wall, the poles, and the cross wall of the four classes of exponentially growing bacteria*[a]

Determinants	Class I	Class II	Class III	Class IV[b]
Cylindrical cell wall	23.23 ± 2.58	28.30 ± 2.26	23.81 ± 1.16	26.61 ± 4.16
Poles	21.92 ± 2.08[c]	22.92 ± 3.84	20.25 ± 2.76	22.44 ± 4.00
	30.05 ± 3.16[d]			
Cross wall		26.17 ± 4.34	33.02 ± 3.00	34.93 ± 4.76

[a] Measurements were done on longitudinal thin sections.
[b] Considered as single cells.
[c] Thin pole.
[d] Thick pole.

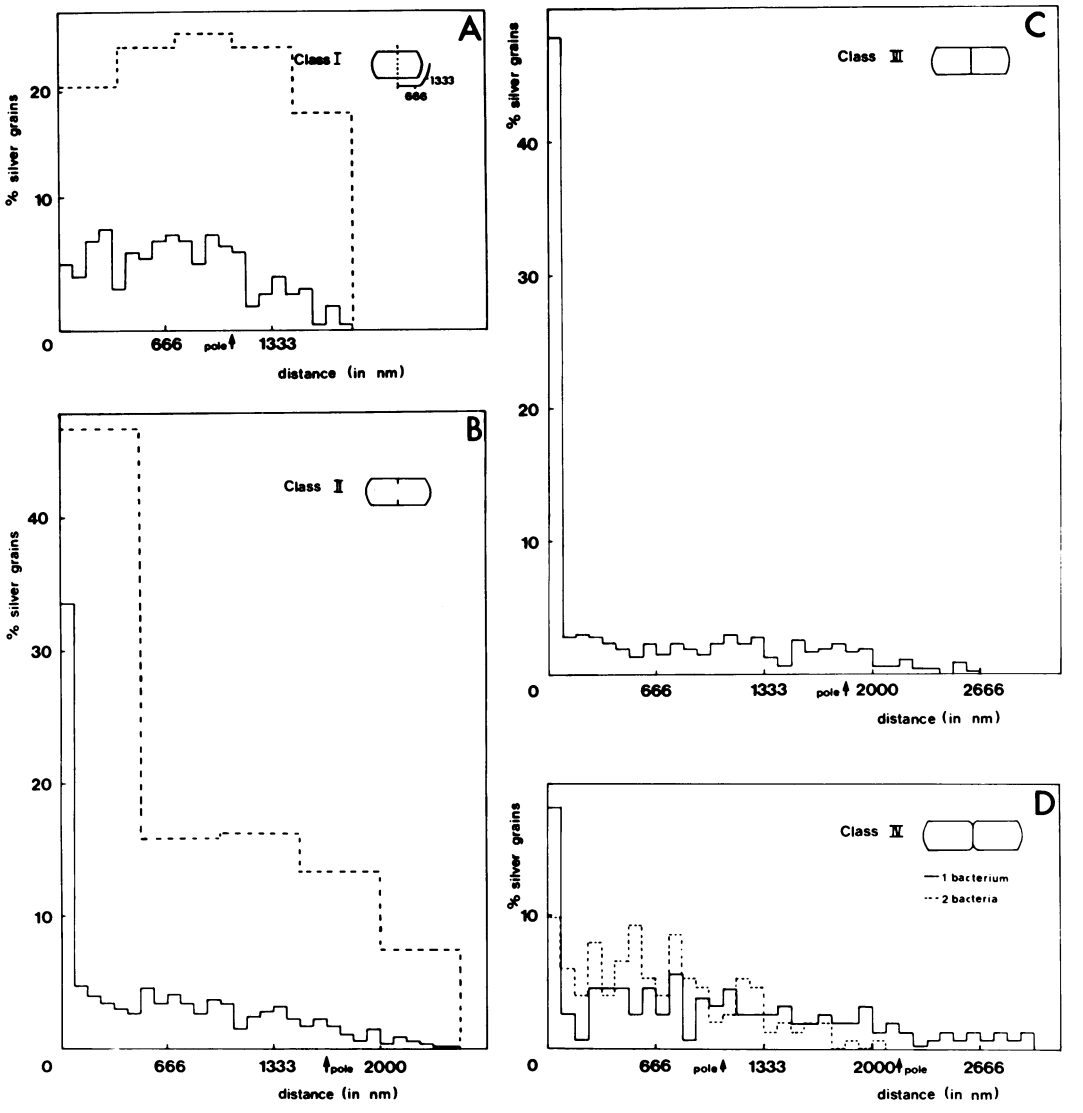

FIG. 6. *Silver grain distribution histograms along the cell wall obtained on thin sections of exponentially growing bacteria with respect to the middle of bacteria (transversal axis of symmetry). The insert in (A) shows this reference line (dotted line). It also shows to which part of the cell wall the distances given in the histograms correspond. Longitudinal sections of bacteria labeled for 2 min with ^{3}H-labeled DAP were analyzed after 32 days of autoradiography. Histograms were prepared in distance steps of 83.3 nm (2.5 mm at G = ×30,000). Quantities of silver grains are expressed as percentages of the total number of cell wall silver grains. The poles are the rounded ends of the thin sections. The arrow indicates the mean distance from the reference line at which the cell wall starts to curve. (A) Class I (solid line); (B) class II (solid line); (C) class III; (D) class IV, solid line: one bacterium; dotted line: two bacteria. Thin sections (30 to 50) of each class were analyzed. This represents 200 to 550 silver grains per class. In classes I and II the distribution of silver grains with respect to the middle of bacteria was also determined after dividing each thin section into five equal parts on each side of the reference line (dotted lines in A and B).*

least partially, the presence of an eventual growth zone because of the size range of the thin sections of a given class. This variation of size could produce the spreading of a growth zone, especially if it is located near the poles of the cells. Therefore, a control was made in the following way for bacteria of classes I and II. Each longitudinal thin section previously analyzed was divided into five equal portions on each side of the reference line (middle of the

cell). The number of silver grains along the cell wall was determined for each of these portions. The results of such an analysis are given in the histograms of Fig. 6A and B (dotted lines). They confirm the results already obtained. Indeed, except for the peak at the forming cross wall (Fig. 6B) no other growth zones appeared. The cylindrical part of the cell wall stayed uniformly labeled.

Autoradiography of thin sections of germinating spores. These young bacteria showed no sign of cellular division and were in the course of their first nuclear division. They were separated into three classes according to their length (Table 5), which ranged from 1.6 to 2.8 μm. Electron micrographs (Fig. 7) show thin sections of cells with a homogeneously labeled cell wall and a highly labeled cytoplasm. As for exponentially growing bacteria, the quantitative distribution of silver grains was established by two ways.

(i) Localization of silver grains in the whole cell. The number of silver grains on the cylindrical part of the wall, on the poles, and in the cytoplasm was established for each class of bacteria. The results are given in Table 5. The average total radioactivity per thin section of bacterium increased as cells elongated. Indeed, when the length of cells increased 1.44-fold between classes I and III, the radioactivity in the cylindrical part of the cell wall and in the cytoplasm increased 1.70-fold, whereas it remains stable at the poles.

The rate of DAP incorporation per micron of cell wall (Table 6) was always lower in the poles than along the cylindrical portion. Measurements of the thickness of the wall (Table 7) showed a clear increase between class I and class III, which probably reflects the maturation of the wall of these young bacteria. Curiously enough however, the wall of class I germinating cells was as thick as the one of exponentially growing bacteria, and it became 30% thicker in class III germinating cells.

(ii) Silver grain distribution along the cell wall. The distribution of silver grains along the cell wall was analyzed for the three classes of germinating cells in the same way as for exponentially growing bacteria. The results are presented in Fig. 8. No prominent peaks of radioactivity appeared in either class of germinating cells. The small peaks appearing along the cylindrical part of the cell wall most probably corresponded to experimental fluctuations. Poles of cells which were just emerging from the spore (class I) were nearly as much labeled as the cylindrical part of the cell wall. Then, as cells elongated, poles became progressively less labeled. This has already been shown by the data in Table 6.

DISCUSSION

The analyses of these autoradiographs show that the only zone of highly localized DAP incorporation is found at the cross wall during its formation. It contains about 50% of the whole cell wall radioactivity in class III exponentially growing bacteria. On thin sections of whole bacteria this growth zone is very narrow, about 0.17 μm wide. When bacteria have no cross wall, as in class I exponentially growing cells or in the three classes of germinating cells, this peak does not appear. Because of its narrowness and its absence when the cross wall is not being synthesized, it seems clear that this peak is involved in cross wall formation only and not in cell wall elongation.

On whole isolated cell walls this peak is not as sharp, being 0.4 to 0.6 μm wide. This is certainly due to the flattening of the cell walls on the collodion film. Moreover, there are never more than 30% of the silver grains in this zone. On thin sections of isolated cell walls the percentage of silver grains in this zone is 36%. This lower percentage as compared to the one found on sections of bacteria is certainly due to the loss of immediate precursors during the breaking of cells. These immediate precursors, such

TABLE 5. *Description of the three classes of thin sections of germinating cells*[a]

Determinants	Class I (1.6–2 μm)[b]		Class II (2–2.5 μm)[b]		Class III (2.4–2.8 μm)[b]	
	M	%	M	%	M	%
Cylindrical cell wall	3.80	32.46	5.43	33.78	6.07	35.27
Poles	2.54	21.71	3.05	18.92	2.29	13.33
Cytoplasm	5.36	45.83	7.60	47.30	8.95	51.40

[a] Results shown as mean (M) number of silver grains and as percentage of the total. Number of thin sections analyzed: class I, 39; class II, 46; class III, 27. Total number of silver grains considered: class I, 247; class II, 390; class III, 226.

[b] Length of thin section.

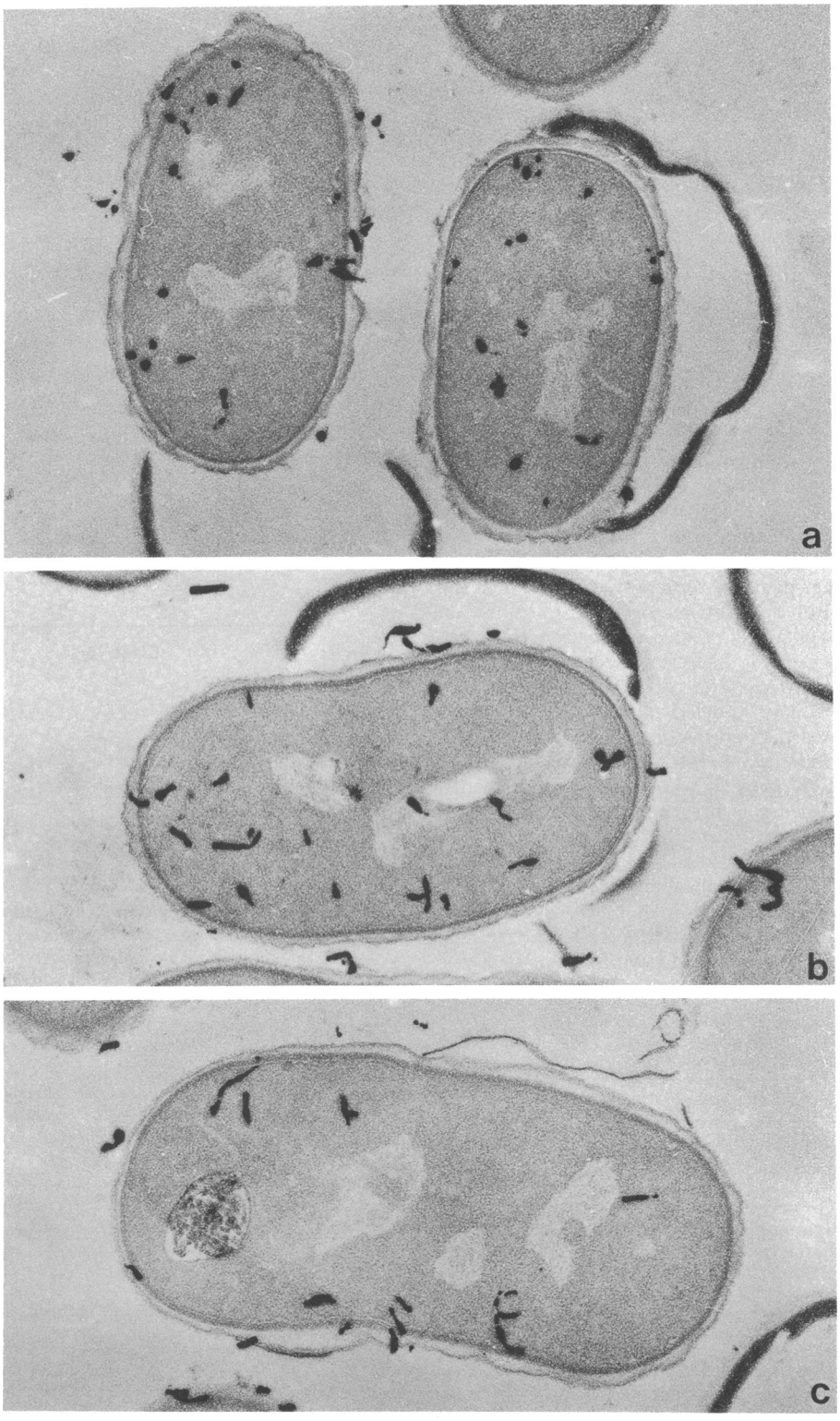

FIG. 7. *Autoradiography of longitudinal thin sections of germinating cells labeled for 2 min with ^{3}H-labeled DAP (42 days of autoradiography). These thin sections represent the three different classes determined according to their length.* (a) *Class I;* (b) *class II;* (c) *class III.* ×30,000.

as dissacharide-pentapeptides, are expected to be at or very near to their site of incorporation into the cell wall. They could be responsible for the higher number of silver grains counted on thin sections of whole bacteria at the cross wall.

Class I isolated cell walls already contain a central peak at the site of cross wall formation which is not found on class I thin sections of whole bacteria. This is due to the fact that isolated cell walls were divided into three classes, whereas thin sections were divided into four classes, and that many class I isolated cell walls have a cross wall in formation. Also, during the analysis of isolated cell walls, the smaller cell walls were most probably discarded because one of their poles was broken or missing. Indeed, the length of the smallest cell wall is more than half of the largest. As shown below, this fragility is due to the incomplete maturation of the new pole issued from the cleavage of the cross wall.

No other peaks of radioactivity appear in the silver grain distribution patterns obtained on isolated cell walls or on thin sections of exponentially growing bacteria or germinating cells. On the contrary, the cell wall is always very homogeneously labeled along its cylindrical part. Since histograms obtained with thin sections of bacteria present the same pattern of distribution as with whole isolated cell walls, murein precursors present near the cell wall in thin sections do not introduce important errors.

This distribution seems to indicate that elongation of the cell wall of *B. megaterium* occurs by diffuse intercalation of newly synthesized murein into the expanding cell wall during exponential growth and germination. It seems highly improbable that this homogeneous dis-

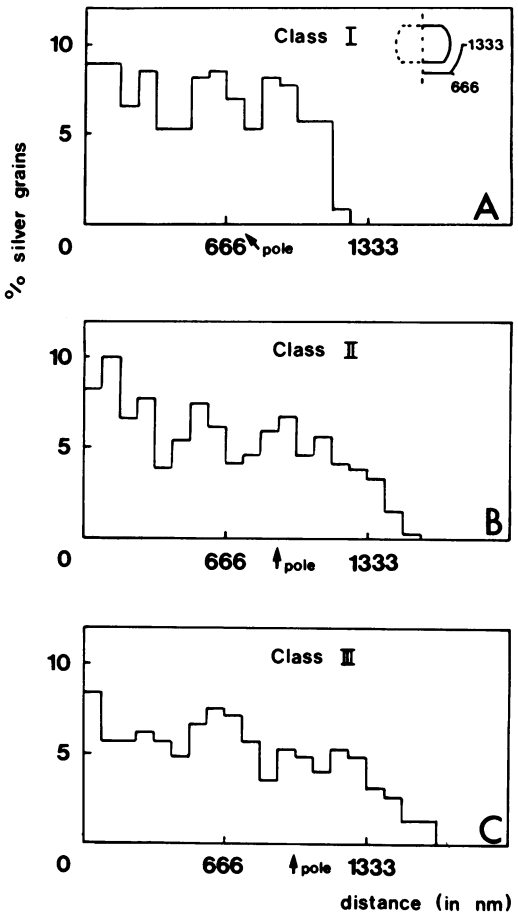

FIG. 8. *Silver grain distribution histograms along the cell wall of germinating bacteria with respect to the center of bacteria. The insert in (A) shows this reference line (dotted line). It also shows to which part of the cell wall the distances given in the histograms correspond. Longitudinal thin sections of bacteria labeled for 2 min with ^{3}H-labeled DAP were analyzed after 42 days of autoradiography. Histograms were prepared in distance steps of 83.3 nm (2.5 mm at G = ×30,000). Quantities of silver grains are expressed as percentages of the total number of cell wall silver grains. The poles are the rounded ends of the thin sections. The arrow indicates the mean distance from the reference line at which the cell wall starts to curve. (A) Class I; (B) class II; (C) class III. Several (27 to 46) sections were analyzed in each class. This represents 226 to 390 silver grains per class.*

TABLE 6. *Number of silver grains per micron of cell wall counted on thin sections of germinating bacteria*[a]

Determinants	Class I	Class II	Class III
Cylindrical cell wall	1.56	1.70	1.48
Poles	1.27	1.35	0.93

[a] The total number of silver grains counted in each class along the cell wall was: class I, 247; class II, 390; class III, 226.

TABLE 7. *Thickness (in nanometers) of the cylindrical part of the cell wall and the poles of the three classes of germinating cells. Measurements were done on longitudinal thin sections*

Determinants	Class I	Class II	Class III
Cylindrical cell wall	24.41 ± 3.00	33.63 ± 3.16	37.22 ± 2.58
Poles	19.25 ± 2.00	28.60 ± 3.74	32.03 ± 1.92

tribution could be due to a rearrangement of the murein molecules in the cell wall since the labeling time corresponds to 0.025 or 0.05 of the doubling time. In contrast, turnover could partially mask eventual growth zones. However, it seems very unlikely that the complete absence of zones, even broad, could be due to turnover only. These results confirm those obtained by Mauck et al. (25) and those obtained in different gram-positive bacteria after thickening of the cell wall (2, 8, 15). They are also in good agreement with biochemical data of Mauck and Glaser (26). By contrast it is more difficult to relate them with observations made by Mendelson and Reeve (27) in a thermosensitive mutant of *Bacillus subtilis* which loses its cylindrical shape at high temperature. After a temperature shift up these authors observed an alteration in cell chains of the cell shape in one or two well-defined regions only, suggesting a zonal growth of the cell wall. It is not excluded however that in this mutant the cell wall defect occurs preferentially at the most active growth sites, such as the cross wall, and then spreads outwards on both sides of these regions. A phenomenon of this type has been described by Highton and Hobbs in *Bacillus cereus* grown in the presence of low concentrations of penicillin (21).

We can also point out that the growth pattern found in *B. megaterium* is very different from the one observed recently in a gram-negative bacterium, *E. coli*. In the latter, growth of the murein layer seems to occur in some defined areas (29; Schwarz et al., submitted for publication). This is not extremely surprising since the cell wall of gram positives and gram negatives are very different in their chemical composition and their structure.

Analyses done have shown that DAP incorporation is particularly high in the poles of germinating cells and in the poles of class I exponentially growing bacteria. Measurements of the thickness of the cell wall indicate that, in these states, the cell wall is not yet mature and is still thickening. However, even in class II, III, and IV exponentially growing cells, the DAP incorporation rate per micron in the poles is not negligible since it represents about 50% of the one found along the cylindrical part. This radioactivity can be attributed either to growth or to turnover. It most unlikely corresponds to real growth leading to elongation. Indeed, in a previous study we had observed that the cell wall polar ends of bacteria treated with chloramphenicol remained thick after recovery of growth, for at least one generation, whereas the cylindrical part became very quickly thinner (15).

On the contrary, turnover in poles is much more probable, especially as Fan et al. (14) have found turnover in polar caps of *B. subtilis*.

Our observations also give new information on the rate of DAP incorporation during the life cycle. It was shown (Table 2) that the total radioactivity, incorporated into the bacterium during the pulse, increases with the length of the cell and doubles between class I and class IV. Such an increase was already observed in *E. coli* (17, 29, 32), but in these studies it was not possible to know whether this increase was due to cell septation only or also to cell elongation. In the experiments we have done with *B. megaterium*, it is possible to visualize the exact location of the radioactive molecules in the different parts of the cell. It is clear that DAP incorporation in the cylindrical part of the cell wall doubles between class I and class IV as a function of the cell length. By contrast it remains unchanged in the poles. And since the thickness of the cylindrical wall remains unchanged, this means that cellular elongation is not constant during the life cycle but increases with the length of the cell. This increase is particularly high just before the cleavage of daughter cells, but is weaker during the formation of the cross wall as if this area of very active growth drained a great amount of murein precursors.

The increase of radioactivity is also found in the cytoplasm. This is quite normal since it seems to correspond to murein precursors and not to free DAP molecules (13).

A similar phenomenon also occurs in germinating cells. At first sight, it seems even more pronounced since the radioactivity in the cylindrical part of the wall is 1.7-fold higher in class III than in class I for an increase in length of only 1.4. This can easily be explained by the thickening of the wall observed in these young bacteria.

Therefore cell elongation is not constant during the life cycle and is greatly accelerated towards its end. This confirms conclusions drawn by Collins and Richmond from their analysis of the cell size frequency in a nonsynchronized culture (12). This mode of growth implies that at the end of a division cycle the two daughter bacteria already possess the number of growth sites they will need after their separation. If this number had remained constant during the whole life cycle, daughter bacteria would possess only half of the needed sites and would have to suddenly double this

number after separation. Thus it seems that the increase in the number of growth sites is independant of the septation process.

ACKNOWLEDGMENTS

We wish to thank Claudine Elmerich and Jean-Paul Aubert for their kind help in isolating the DAP⁻ Lys⁻ mutant.

This work was supported by grants from the Délégation Générale à la Recherche Scientifique et Technique (research grant 71-7-3082), from the Centre National de la Recherche Scientifique (Laboratoire associé n° 88), and from the Commissariat à l'Energie Atomique.

LITERATURE CITED

1. Aubert, J. P., J. Millet, E. Pineau, and G. Milhaud. 1961. L'acide N-succinyl-L-glutamique chez *Bacillus megaterium* en voie de sporulation. Biochim. Biophys. Acta **51**:529-537.
2. Boothby, D., L. Daneo-Moore, M. L. Higgins, J. Coyette, and G. D. Shockman. 1973. Turnover of bacterial cell wall peptidoglycans. J. Biol. Chem. **248**:2161-2169.
3. Briles, E. B., and A. Tomasz. 1970. Radioautographic evidence for equatorial wall growth in a Gram positive bacterium. Segregation of choline-^{3}H-labeled teichoic acid. J. Cell. Biol. **47**:786-790.
4. Caro, L. 1966. Progress in high resolution autoradiography. Progr. Biophys. Mol. Biol. **16**:171-190.
5. Chaloupka, J. 1962. The mucopeptide turnover in the cell wall of growing cultures of *Bacillus megaterium* KM. Experientia **18**:362-364.
6. Chaloupka J. 1967. Synthesis and degradation of surface structure by growing and non growing *Bacillus megaterium*. Folia Microbiol. **12**:264-273.
7. Chaloupka, J., L. Rihova, and P. Kreckova. 1964. Degradation and turnover of bacterial cell wall mucopeptides in growing bacteria. Folia Microbiol. **9**:9-15.
8. Chung, K. L. 1971. Thickened cell walls of *Bacillus cereus* grown in the presence of chloramphenicol: their fate during cell growth. Can. J. Microbiol. **17**:1561-1565.
9. Chung, K. L., R. Z. Hawirko, and P. K. Isaac, 1964. Cell wall replication. I. Cell wall growth of *Bacillus cereus* and *Bacillus megaterium*. Can. J. Microbiol. **10**:43-48.
10. Chung, K. L., R. Z. Hawirko, and P. K. Isaac. 1964. Cell wall replication. II. Cell wall growth and cross wall formation of *Escherichia coli* and *Streptococcus faecalis*. Can. J. Microbiol. **10**:473-482.
11. Cole, R. M., and J. J Hahn. 1962. Cell wall replication in *Streptococcus pyogenes*. Science **135**:722-723.
12. Collins, J. F., and M. H. Richmond. 1962. Rate of growth of *Bacillus cereus* between divisions. J. Gen. Microbiol. **28**:15-33.
13. De Chastellier, C., C. Frehel, and A. Ryter. 1975. Cell wall growth of *Bacillus megaterium*: cytoplasmic radioactivity after pulse-labeling with tritiated diaminopimelic acid. J. Bacteriol. **123**:1197-1207.
14. Fan, D. P., B. E. Beckman, and M. M. Beckmann. 1974. Cell wall turnover of the hemispherical caps of *Bacillus subtilis*. J. Bacteriol. **117**:1330-1334.
15. Frehel, C., A. M. Beaufils, and A. Ryter. 1971. Etude au microscope électronique de la croissance de la paroi chez *Bacillus subtilis* et *Bacillus megaterium*. Ann. Inst. Pasteur (Paris) **121**:139-148.
16. Grandboulan, P. 1965. The use of radioautography in investigating protein synthesis, p. 43-63. *In* J. R. C. Harris (ed.), Symp. Int. Soc. Cell Biol., vol. 4. Academic Press Inc., New York.
17. Hakenbeck, R., and W. Messer. 1974. Activity of murein hydrolases and membrane synthesis in synchronized *Escherichia coli* B/r. Ann. Microbiol. **125**(B):163-166.
18. Higgins, M. L., and G. D. Shockman. 1970. Model for cell wall growth of *Streptococcus faecalis*. J. Bacteriol. **101**:643-648.
19. Higgins, M. L., and G. D. Shockman. 1971. Procaryotic cell division with respect to wall and membranes. Crit. Rev. Microbiol. **1**:29-72.
20. Highton, P. J., and D. G. Hobbs. 1971. Penicillin and cell wall synthesis: a study of *Bacillus licheniformis* by electron microscopy. J. Bacteriol. **106**:646-658.
21. Highton, P. J., and D. G. Hobbs. 1972. Penicillin and cell wall synthesis: a study of *Bacillus cereus* by electron microscopy. J. Bacteriol. **109**:1181-1190.
22. Hughes, R. C., and E. Stokes. 1971. Cell wall growth in *Bacillus licheniformis* followed by immunofluorescence with mucopeptide-specific antiserum. J. Bacteriol. **106**:694-696.
23. Luft, J. H. 1961. Improvements in epoxy-resin embedding methods. J. Biophys. Biochem. Cytol. **9**:409-414.
24. Mauck, J., L. Chan, and L. Glaser. 1971. Turnover of the cell wall of gram positive bacteria. J. Biol. Chem. **246**:1820-1827.
25. Mauck J., L. Chan, L. Glaser, and J. Williamson. 1972. Mode of cell wall growth of *Bacillus megaterium*. J. Bacteriol. **109**:373-378.
26. Mauck, J., and L. Glaser. 1972. On the mode of in vivo assembly of the cell wall of *Bacillus subtilis*. J. Biol. Chem. **247**:1180-1187.
27. Mendelson, N. H., and J. N. Reeve. 1973. Growth of the *Bacillus subtilis* cell surface. Nature (London) New Biol. **243**:62-64.
28. Reynolds, D. M. 1963. The use of lead citrate at high pH as an electron opaque stain in electron microscopy. J. Cell. Biol. **17**:208-213.
29. Ryter, A., Y. Hirota, and U. Schwarz. 1973. Process of cellular division in *Escherichia coli*. Growth pattern of *Escherichia coli* murein. J. Mol. Biol. **78**:185-195.
30. Ryter, A., and E. Kellenberger. 1958. Etude au microscope electronique de plasmas contenant de l'acide désoxyribonucléique. I. Les nucléoides des bactéries en croissance. Z. Naturforsch. **13**:597-605.
31. Salpeter, M. M., L. Bachman, and E. E. Salpeter. 1969. Resolution of electron microscope autoradiography J. Cell. Biol. **41**:1-32.
32. Schwarz, U., A. Asmus, and H. Frank. 1969. Autolytic enzymes and cell division of *Escherichia coli*. J. Mol. Biol. **41**:419-429.
33. Swanson, J., K. C. Hsu, and E. C. Gotschlitch. 1969. Electron microscopic studies on streptococci. I. M. antigen. J. Exp. Med. **130**:1063-1075.
34. Wagner M. 1964. Studien mit fluoreszierenden antikorpern an wachsenden bakterien. I. Die neulbildung der zellwand bei *Diplococcus pneumoniae*. Zentralbl. Bakteriol. Parasitenkd. Infektionskr. Hyg. Abt. 1 Orig. **195**:87-94.